How noise can generate calcium spike-type oscillations in deterministic equilibrium modes

Irina Bashkirtseva* and Lev Ryashko†
Institute of Natural Sciences and Mathematics, Ural Federal University, Lenina 51, Ekaterinburg, Russia

(Received 21 January 2022; revised 13 March 2022; accepted 20 April 2022; published 9 May 2022)

Stochastic excitability of spiking oscillatory regimes in the calcium kinetics is studied on the basis of the Li-Rinzel conceptual model. The probabilistic mechanisms of the noise-induced generation of large-amplitude oscillations in parametric zones, where the original deterministic model has only stable equilibria, are investigated numerically and analytically. A parametric statistical description of interspike intervals is curried out and the phenomenon of coherence resonance is discussed. For the analytical study of the stochastic excitement, the confidence domain method using a stochastic sensitivity technique is applied. In this analysis, a key role of mutual arrangement of the confidence ellipses and separatrices detaching the sub- and supercritical regions is demonstrated. It is shown that in the Li-Rinzel model such separatrices are the stable manifolds of the saddle equilibria and the transient semiattractors.

DOI: 10.1103/PhysRevE.105.054404

I. INTRODUCTION

In a wide range of intra- and intercellular processes, a change in calcium concentration plays an important role [1,2]. Regular and irregular calcium oscillations were reported in many papers on experimental studies [3–6]. Elucidation of underlying mechanisms of occurrence of calcium oscillations attracts the attention of researchers, both biophysicists and mathematicians. In theoretical studies of calcium dynamics, mathematical models in a form of differential equations are widely used [7–10].

It has been shown that key experimental observations can be captured by minimal models consisting of two dynamical variables such as the Li-Rinzel [11] or the Dupont-Goldbeter [12] models. In initial papers on mathematical studies of calcium dynamics, an appearance of calcium oscillations was explained by the existence of limit cycles in deterministic models. Various types of limit cycles were studied in connection with analysis of encoding of external stimuli in amplitude and frequency modulation of intracellular calcium oscillations [13].

An important step in the study of calcium dynamics is associated with stochastic aspects. Indeed, cellular processes are subject to random disturbances of a different nature [14,15]. It is well known that in nonlinear systems noise can induce a wide variety of stochastic phenomena, such as noise-induced transitions [16–18], stochastic resonance [19,20], noise-induced chaos [21,22], stochastic excitability, and coherence resonance [23–26]. Stochastic excitability plays a special role in understanding the mechanisms of neural activity [27–31].

A constructive role of noise in the generation of calcium oscillations is a subject of many papers (see, e.g., [32–37]). Phenomena of stochastic and coherent resonances in models of calcium oscillations were studied numerically in [38–41].

When clarifying the underlying mechanisms of stochastic effects in strongly nonlinear dynamical systems, it is important to take into account peculiarities of phase portraits of the initial deterministic model and the sensitivity of attractors to random forcing [23,42,43].

The present paper aims to study how this interplay of nonlinearity and stochasticity causes noise-induced generation of calcium oscillations in parameter zones of stable equilibria. On the basis of the conceptual model proposed by Li and Rinzel [11], we demonstrate the effects of stochastic excitement of spike-type calcium oscillations, and perform numerical and analytical studies.

In Sec. II, we present the results of the bifurcation analysis of the equilibrium and oscillatory modes of the deterministic system and discuss the peculiarities of phase portraits.

In Sec. III, we show how random disturbances in the flux J_{chan} can generate spike-type calcium oscillations in the equilibrium parameter zones of the unforced Li-Rinzel model. Here, the statistics of interspike intervals makes it possible to reveal the occurrence of stochastic excitement and to find the intensity of the noise associated with the coherence resonance. To clarify mechanisms of these noise-induced phenomena, we apply an analytical approach which uses the stochastic sensitivity of equilibria and method of confidence domains [44,45].

II. DETERMINISTIC MODEL

As a deterministic skeleton of our study, we use the Li-Rinzel model [11,32] of calcium dynamics:

$$\frac{dc}{dt} = J_{\text{chan}} + J_{\text{leak}} - J_{\text{pump}}, \quad \frac{dh}{dt} = \frac{h_\infty - h}{\tau_h},$$
$$J_{\text{chan}} = v_1 m_\infty^3 h^3 [c_0 - (1 + c_1)\, c],$$

*Irina.Bashkirtseva@urfu.ru
†Corresponding author: Lev.Ryashko@urfu.ru

$$J_{\text{leak}} = v_2[c_0 - (1+c_1)\,c], \quad J_{\text{pump}} = \frac{v_3 c^2}{K_3^2 + c^2},$$
$$m_\infty = \frac{pc}{(p+d_1)(c+d_5)}, \quad h_\infty = \frac{Q_2}{Q_2+c},$$
$$\tau_h = \frac{1}{a_2(Q_2+c)}, \quad Q_2 = \frac{p+d_1}{p+d_3}\,d_2. \tag{1}$$

The dynamical variables of the Li-Rinzel model (1) are the free cytosolic Ca^{2+} concentration c and the fraction h of the open inositol trisphosphate IP_3 receptor subunits.

The dynamics of the calcium concentration c is governed by three fluxes: a passive leak of Ca^{2+} from the endoplasmic reticulum to the cytosol, J_{leak}; an active uptake of Ca^{2+} into the endoplasmic reticulum due to action of the pumps, J_{pump}; and Ca^{2+} release J_{chan} that is mutually gated by Ca^{2+} and the inositol trisphosphate IP_3 concentration p. Because the IP_3 concentration p plays an important role in the variation of regimes of the model (1), we use p as a control parameter.

Here, we follow [13] in notations and choice of fix values of parameters as

$$v_1 = 6\ \text{s}^{-1}, \quad v_2 = 0.11\ \text{s}^{-1}, \quad v_3 = 0.9\ \mu\text{M}\,\text{s}^{-1},$$
$$c_0 = 2\ \mu\text{M}, \quad c_1 = 0.185, \quad d_1 = 0.13\ \mu\text{M},$$
$$d_2 = 1.049\ \mu\text{M}, \quad d_3 = 0.9434\ \mu\text{M}, \quad d_5 = 0.082\,34\ \mu\text{M},$$
$$a_2 = 0.2\ \mu\text{M}^{-1}\,\text{s}^{-1}.$$

As for the parameter K_3, in [13] two cases were compared. The value $K_3 = 0.1\ \mu$M, as in the initial paper [11], corresponds to the "amplitude modulation" of calcium oscillations where the frequency is almost constant. Stochastic effects in the Li-Rinzel model with $K_3 = 0.1\ \mu$M are well studied (see, e.g., [32,33,37]). The value $K_3 = 0.051\ \mu$M corresponds to the qualitatively different so-called "frequency modulation" [13] in the intracellular calcium oscillations with the almost constant amplitude. This is an excitable version of the Li-Rinzel model.

In the present paper, we focus on this excitable version with $K_3 = 0.051\ \mu$M. Note that this value belongs to the parametric zone of frequency modulation determined in [13]. Moreover, in [13] one can find (c_0, K_3)-parameter domains corresponding to "amplitude" and mixed-type modulation.

To find equilibria, we have to solve the system $\dot{c} = 0$, $\dot{h} = 0$. The equation $\dot{h} = 0$ gives $h(c) = Q_2/(Q_2 + c)$. Substituting this expression to the equation $\dot{c} = 0$, we get the equation $\varphi(c) = J_{\text{chan}}(c, h(c)) + J_{\text{leak}}(c) - J_{\text{pump}}(c) = 0$. In Fig. 1, plots of the function $\varphi(c)$ are shown for various values of the parameter p. Roots of the equation $\varphi(c) = 0$ determine c coordinates of the equilibria of the system (1).

As can be seen, the system (1) can possess three equilibria: $M_1(\bar{c}_1, \bar{h}_1)$, $M_2(\bar{c}_2, \bar{h}_2)$, and $M_3(\bar{c}_3, \bar{h}_3)$ $(\bar{c}_1 < \bar{c}_2 < \bar{c}_3)$. A description of dynamical regimes of the system (1) for $0.1 < p < 1.5$ is given by the bifurcation diagram in Fig. 2 with details in enlarged fragments. Here, six bifurcation points are marked: $p_1 = 0.479$, $p_2 = 0.509\,228\,454\,511\,9$, $p_3 = 0.5098$, $p_4 = 0.5258$, $p_5 = 0.855$, and $p_6 = 1.1164$.

In the interval $0.1 < p < p_1$, the system (1) has a unique equilibrium M_1. In the interval $p_1 < p < p_4$, the system has three equilibria M_1, M_2, and M_3. In the interval $p_4 < p < 1.5$, the system has the only equilibrium M_3. The equilibrium M_1 is stable in the interval $0.1 < p < p_3$. The equilibrium M_2 is always unstable, whereas M_3 is stable for $p_5 < p < 1.5$. In Fig. 2, the stable equilibria are marked by blue solid lines, and unstable equilibria are shown by red dashed lines.

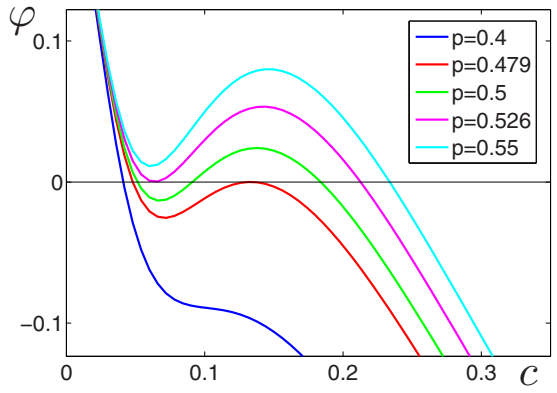

FIG. 1. Plots of the function $\varphi(c)$.

In the interval $p_2 < p < p_6$, the system (1) exhibits the stable limit cycles. In Fig. 2, extrema of the c coordinates of these cycles are plotted by green solid lines. Here, p_2 and p_6 are saddle-node bifurcation points.

So, the system (1) exhibits parameter zones of mono- and bistability. Intervals $0.1 < p < p_2$ and $p_6 < p < 1.5$ are monostability zones with stable equilibria, M_1 or M_3, correspondingly. The interval $p_3 < p < p_5$ is the monostability zone with the stable limit cycle as a single attractor.

In the intervals $p_2 < p < p_3$ and $p_5 < p < p_6$, this cycle coexists with the stable equilibria M_1 or M_3, correspondingly. In these bistability intervals, the limit cycle is separated from the stable equilibrium by the unstable limit cycle (extrema of c coordinates of the unstable cycles are plotted by red solid lines).

The variety of dynamical behavior of the deterministic system (1) is illustrated by phase portraits in Fig. 3. For $p = 0.5$ [see Fig. 3(a)], the system (1) has three equilibria. The equilibrium M_1 (filled circle) is stable, and M_2, M_3 (empty circles) are unstable. Here, the stable manifold of the saddle point M_2 (green dashed) plays an important role of the separatrix in the transient processes. All trajectories tend to M_1 but in different ways: trajectories starting below the green curve promptly tend to M_1 while trajectories starting above this green curve exhibit long-amplitude excursion before approaching M_1. The location of this separatrix will be used below in the analysis of stochastic excitement.

For $p = 0.51$ [see Fig. 3(b)], all three equilibria are unstable, and trajectories tend to the orbit of the stable limit cycle (thick blue curve). For $p = 1$ [see Fig. 3(c)], the single equilibrium M_3 (filled circle) is stable. Along with this attractor, the system (1) exhibits a stable limit cycle (thick blue curve). Basins of these attractors are separated by the orbit of the unstable cycle (red dashed curve).

For $p = 1.12$ [see Fig. 3(d)], all trajectories tend to the unique stable equilibrium M_3. Here, two various transient processes can be determined. For small deviations of the initial state from M_3, the solution uniformly in a spiral approaches

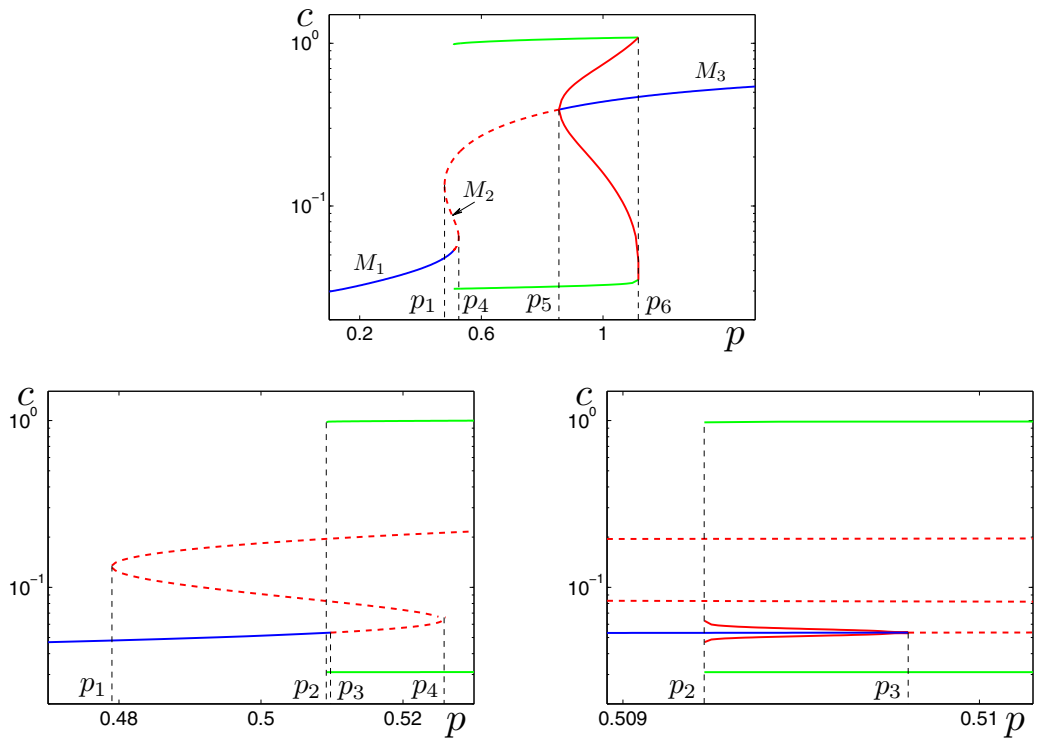

FIG. 2. Bifurcation diagram with the enlarged fragments. Bifurcation values are $p_1 = 0.479$, $p_2 = 0.509\,228\,454\,511\,9$, $p_3 = 0.5098$, $p_4 = 0.5258$, $p_5 = 0.855$, $p_6 = 1.1164$.

the point M_3. If the initial deviation is rather large, then the trajectory has a fragment that looks like a closed curve, similar to the orbit of the limit cycle [compare with Fig. 3(c)]. This transient fragment can be specified as a transient semiattractor.

Within the framework of deterministic models, the experimentally observed calcium oscillations are explained mathematically by the stable limit cycles. However, the calcium oscillations can appear in the parameter zones where

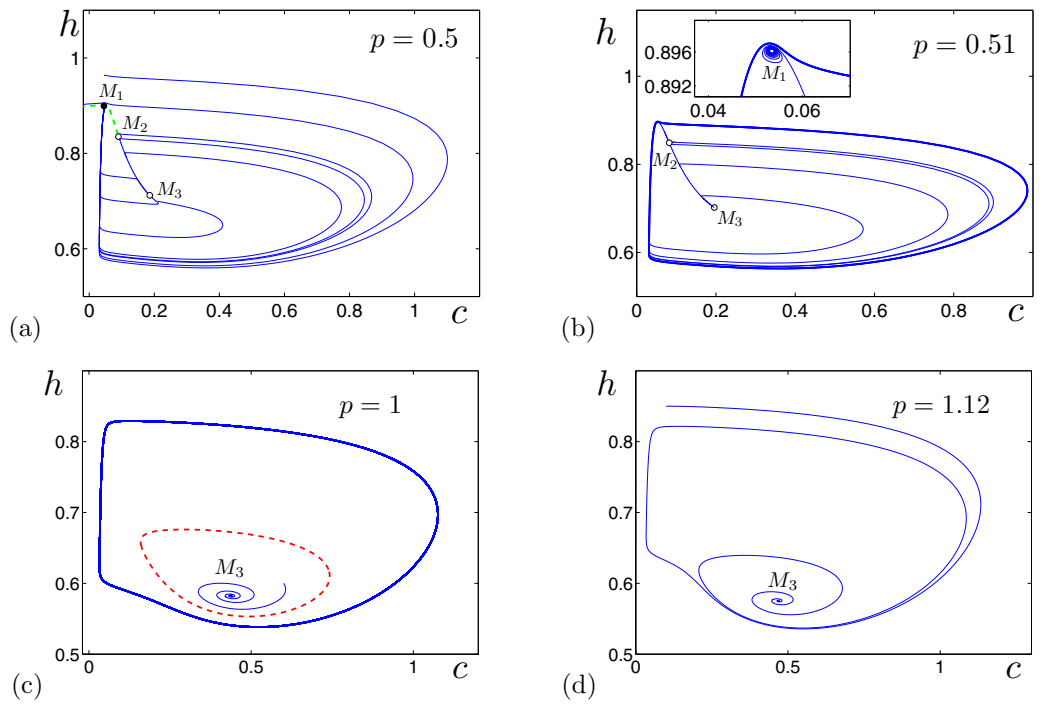

FIG. 3. Phase portraits of the system (1) for (a) $p = 0.5$, (b) $p = 0.51$, (c) $p = 1$, (d) $p = 1.12$.

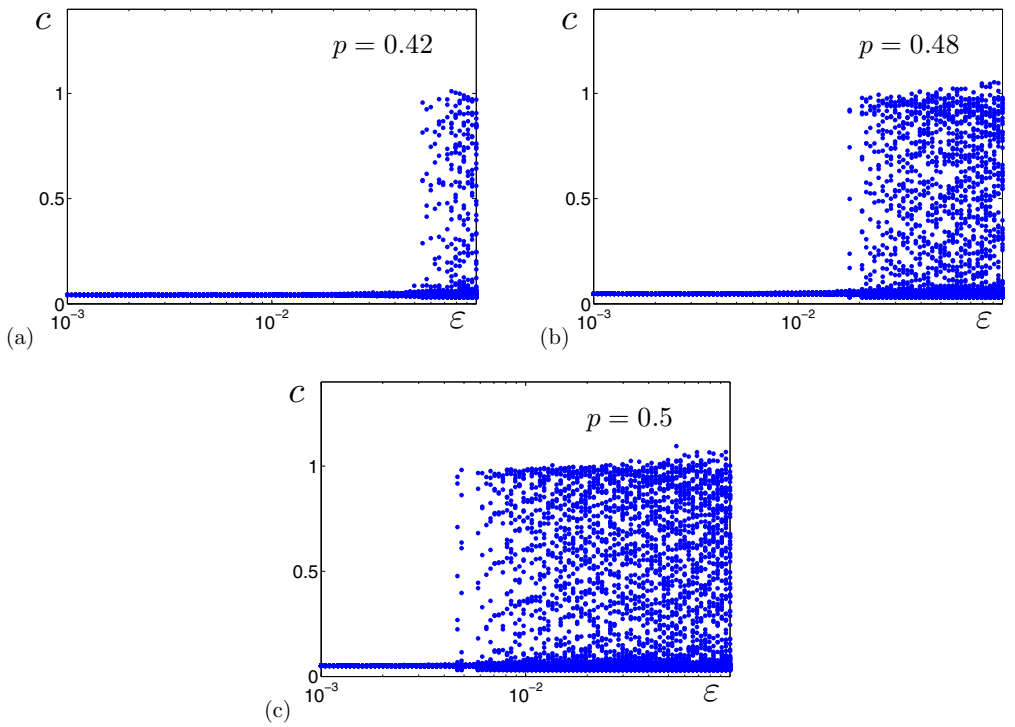

FIG. 4. Random states of the system (2) solutions starting from the equilibrium M_1: (a) for $p = 0.42$, (b) for $p = 0.48$, and (c) for $p = 0.5$.

the deterministic model predicts the stable equilibrium modes only. The reason for the appearance of large-amplitude oscillations can be in even weak stochastic disturbances accompanying any real process. The phenomenon of such stochastic excitement of calcium oscillations is studied in the following section.

III. STOCHASTIC MODEL

In the study of noise-induced phenomena in calcium dynamics, we will use the following stochastic variant of the Li-Rinzel model:

$$\frac{dc}{dt} = J_{\text{chan}}^{\text{noise}} + J_{\text{leak}} - J_{\text{pump}}, \quad \frac{dh}{dt} = \frac{h_\infty - h}{\tau_h}. \tag{2}$$

Here, we take into account parametric random disturbances in the J_{chan}: $v_1 \to v_1[1 + \varepsilon\xi(t)]$, where $\xi(t)$ is a white Gaussian noise with parameters $\langle\xi(t)\rangle = 0$, $\langle\xi(t)\xi(\tau)\rangle = \delta(t - \tau)$, and ε is a scalar parameter of noise intensity. So, in the system (2) we put

$$J_{\text{chan}}^{\text{noise}} = v_1[1 + \varepsilon\xi(t)]m_\infty^3 h^3[c_0 - (1 + c_1)c].$$

In the present paper, we focus on the phenomenon of stochastic excitement in the parameter zones where the deterministic system exhibits the equilibrium as a single attractor. The system (1) has two such zones: $p < p_2$ with the stable equilibrium M_1 and $p > p_6$ with the stable equilibrium M_3 (see Fig. 2).

A. Stochastic excitement in the parameter zone $p < p_2$

Consider an impact of stochastic disturbances in the monostability zone $0.1 < p < p_2$ where the equilibrium M_1 is the only attractor of the system (1).

In Fig. 4, random states of the stochastic system (2) solutions starting from the stable equilibrium M_1 are plotted for three values of the parameter p versus noise intensity ε. Here, we present the results of direct numerical simulation of random solutions found by the Euler-Maruyama scheme with the time step 0.001. In Fig. 4, for any ε, we plot states of the continuous variable c after the transient interval [0,500] in the Poincaré sections with temporal discretization $T = 1$.

For weak noise, random solutions of the system (2) slightly oscillate near M_1, but at the certain threshold noise intensity a behavior of the system abruptly changes, namely, the dispersion of random states sharply increases. Such a behavior is typical for the excitable systems. Note that the corresponding threshold noise intensity depends on the value of p: the closer p to the bifurcation point p_2, the lower this critical noise intensity [compare Figs. 4(a), 4(b) and 4(c)].

Phase trajectories and time series of the system (2) solutions illustrate this stochastic excitement in Fig. 5 for $p = 0.48$ and Fig. 6 for $p = 0.5$ in detail. In Fig. 5(a), phase trajectories of the system (2) solutions with $p = 0.48$ starting from the equilibrium M_1 are shown for $\varepsilon = 0.01$ (red), $\varepsilon = 0.03$ (green), and $\varepsilon = 0.1$ (blue). As one can see, at low noise with $\varepsilon = 0.01$, solutions are localized near the equilibrium M_1. For $\varepsilon = 0.03$, trajectories show large-amplitudes loops and time series are of a spike nature [see Fig. 5(b)] with alternation of small-amplitude noisy oscillations and sharp blowouts in a form of narrow peaks. So, in the Li-Rinzel model, even small random disturbances can generate calcium oscillations of large amplitude.

This phenomenon of stochastic excitement is demonstrated in Fig. 6 for the parameter value $p = 0.5$ that is closer to the bifurcation point p_2. Note that the system generates spike oscillations even for $\varepsilon = 0.01$. Comparing (b) and (c) in Figs. 5

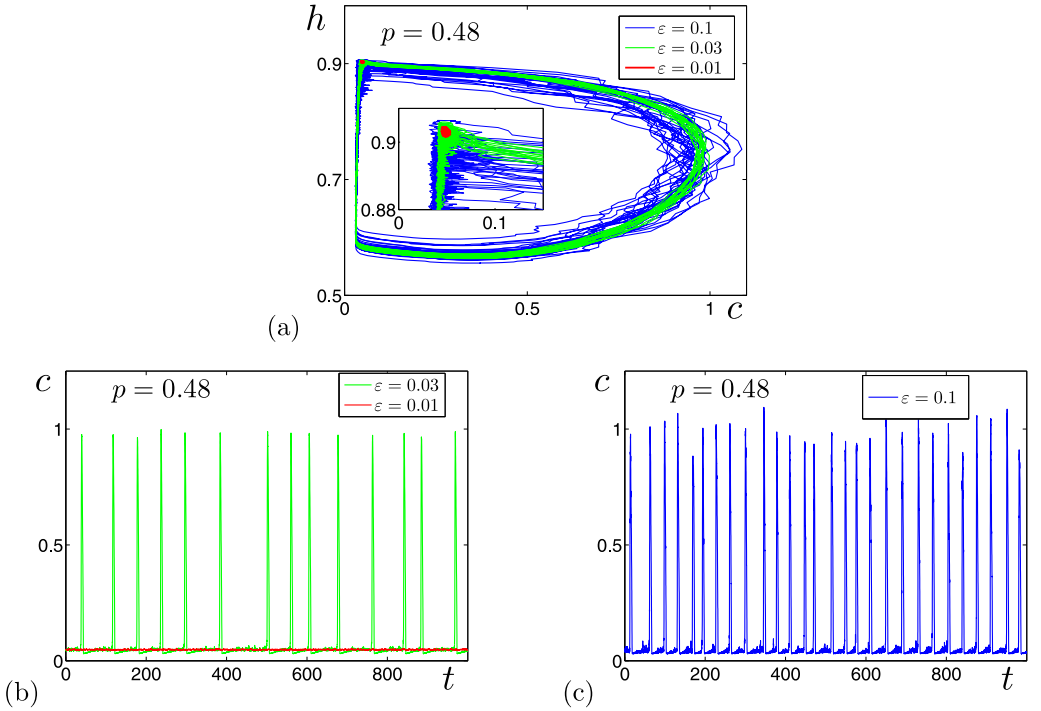

FIG. 5. Random trajectories and time series of the system (2) solutions for $p = 0.48$.

and 6, one can conclude that under increasing noise the intervals between successive spikes decrease.

Details of the statistics of random interspike intervals τ are presented in Figs. 7(a) and 7(b). In Fig. 7(a), plots of mean values $\langle\tau\rangle$ of interspike intervals for various p are shown versus noise intensity ε. A sharp descent in these plots marks the threshold noise intensity corresponding to the onset of generation of spikes. Here, the aforementioned dependence of this threshold on the parameter p is clearly seen. Under increasing noise, after this sharp descent, plots of mean values $\langle\tau\rangle$ monotonously decrease and stabilize.

For comparison, we also plot here a dependence of mean values $\langle\tau\rangle$ for the parameter value $p = 0.6$ (light blue) that corresponds to the limit cycles zone in the deterministic

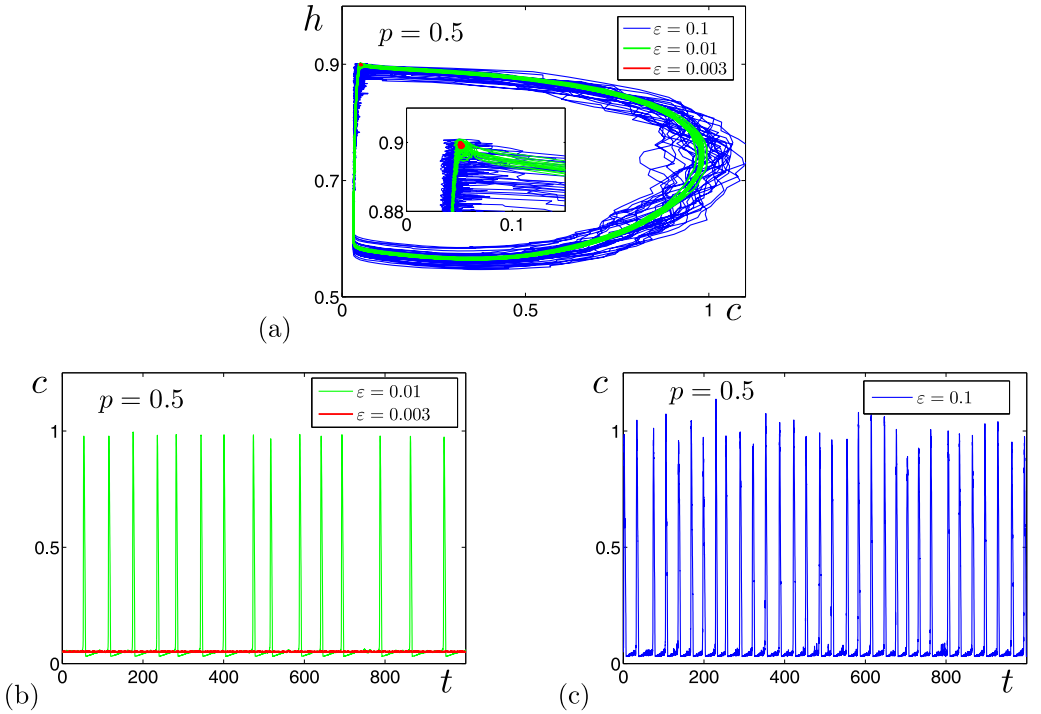

FIG. 6. Random trajectories and time series of the system (2) solutions for $p = 0.5$.

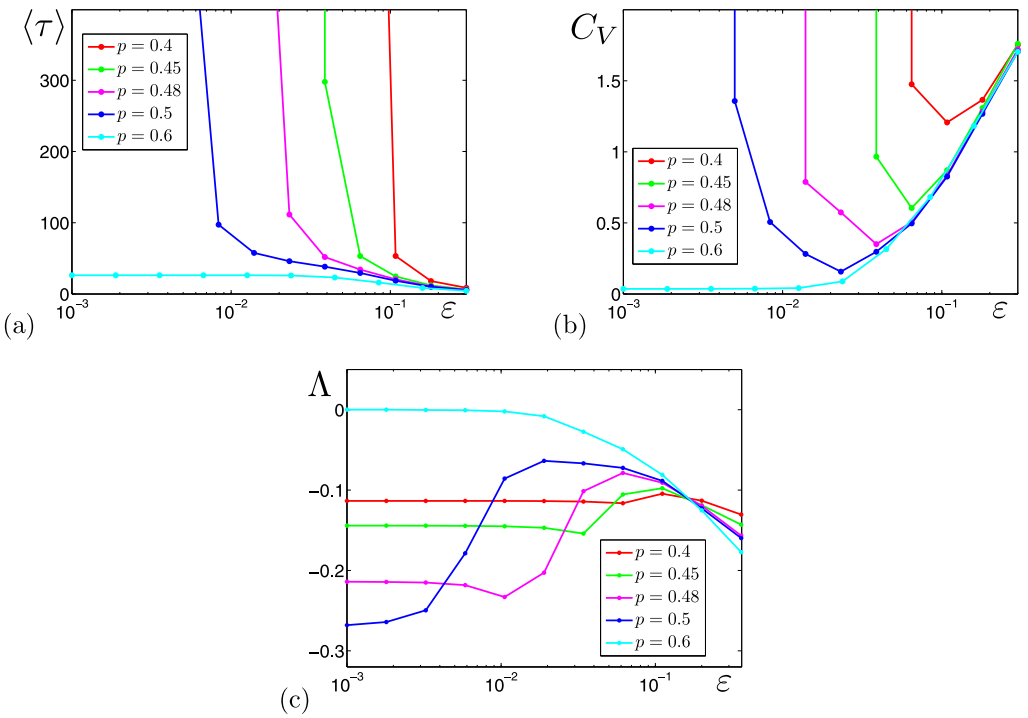

FIG. 7. Stochastic system (2): (a) mean values $\langle\tau\rangle$, (b) coefficient of variation C_V of interpike intervals τ, and (c) largest Lyapunov exponents $\Lambda(\varepsilon)$. Here, minima of C_V in (b) and maxima of Λ in (c) correspond to coherence resonance.

system (1). It is clearly seen, that for strong noise frequency of generated spikes in the parameter zone $p < p_2$ of equilibria is close to the frequency of noisy self-oscillations in the zone $p > p_2$.

In Fig. 7(b), for the same set of the parameter p, plots of the coefficient of variation C_V of interpike intervals τ are shown versus noise intensity ε. These curves have a characteristic feature: for any p, there is a distinct minimum at a certain ε. Such type of behavior determines the important phenomenon of coherence resonance [27]. For p from the monostability zone $0.1 < p < p_2$, the minimum of C_V localizes the value of ε for which noise-induced spiking oscillations are most coherent.

Peculiarities of the internal dynamics of stochastic flows can be characterized by largest Lyapunov exponents Λ that specify the average convergence of random trajectories. In Fig. 7(c), plots of the function $\Lambda(\varepsilon)$ are shown. We calculated the largest Lyapunov exponents by the standard Benettin method [46,47].

For any p, there is an ε zone where increasing noise essentially changes Λ. It should be noted that this characteristic is more sensitive to noise for $p = 0.5$ that is closer to the bifurcation point p_2.

Let us show how the phenomenon of stochastic excitement can be analyzed parametrically by means of a confidence domain technique [42,45]. A key role in this technique is played by the stochastic sensitivity matrix of the equilibrium. The stochastic sensitivity matrix W of the equilibrium of the deterministic system (1) is a unique solution of the equation

$$FW + WF^{\top} + S = 0,$$

where F is a Jacobi matrix of the deterministic system at the equilibrium and the matrix S characterizes the impact of noise. For the equilibrium $M_1(\bar{c}_1, \bar{h}_1)$ in the system (2), we have $S = \mathrm{diag}[J^2_{\mathrm{chan}}(\bar{c}_1, \bar{h}_1), 0]$. Eigenvalues λ_1, λ_2 of the matrix W serve as scalar characteristics of sensitivity of the equilibrium to noise. Plots of $\lambda_1(p), \lambda_2(p)$ for the equilibrium M_1 are shown in Fig. 8. Values of λ_1 and λ_2 differ in several orders and unlimitedly increase approaching the bifurcation point p_3.

Eigenvalues λ_1, λ_2 and eigenvectors u_1, u_2 of the stochastic sensitivity matrix W give a geometrical description of the dispersion of random states around the equilibrium in the form of the confidence ellipse. The equation for such confidence ellipse is written as

$$\frac{z_1^2}{\lambda_1} + \frac{z_2^2}{\lambda_2} = -2\varepsilon^2 \ln(1 - \mathcal{P}),$$

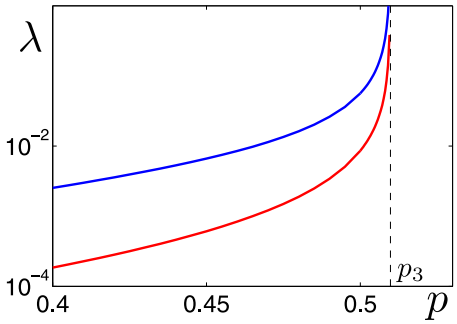

FIG. 8. Eigenvalues λ_1, λ_2 of the stochastic sensitivity matrix W for the equilibrium M_1 versus parameter p.

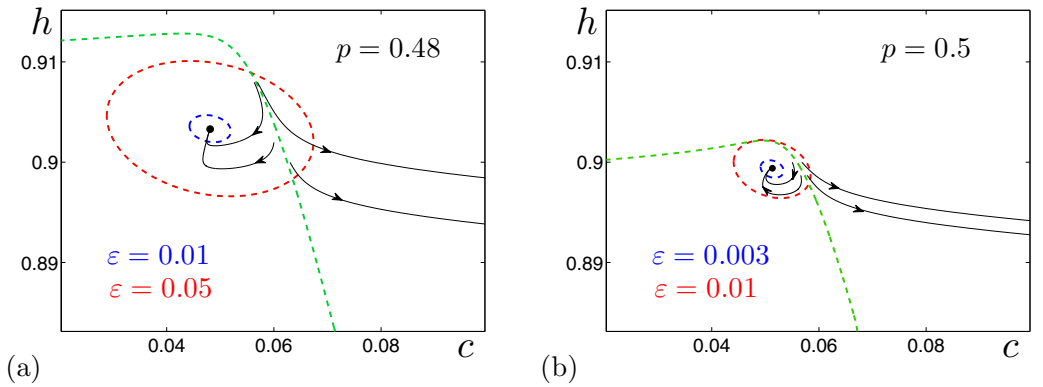

FIG. 9. Confidence ellipses method in the analysis of stochastic excitement. Here, we show the stable equilibrium M_1 (black dot), deterministic trajectories (black curves), confidence ellipses, and stable manifolds (green dashed) of the saddle equilibrium M_2 for (a) $p = 0.48$ and (b) $p = 0.5$.

where z_1, z_2 are coordinates in the basis of u_1, u_2 with the deterministic equilibrium as an origin, the parameter ε is the noise intensity, and $\mathcal{P}$ is the fiducial probability.

The mutual arrangement of confidence domains and separatrices in phase plane can serve as a useful tool in the analysis of various noise-induced transitions [42,45]. Consider how this general approach can be applied to the analysis of noise-induced excitement in the Li-Rinzel model.

In Fig. 9(a), the confidence ellipses are plotted around the equilibrium M_1 (black dot) of the system (2) with $p = 0.48$ for two values of noise intensity: $\varepsilon = 0.01$ (blue dashed) and $\varepsilon = 0.05$ (red dashed). Here, by black we show phase trajectories of the deterministic system, and by green dashed the stable manifold of the saddle equilibrium M_2, which serves as a separatrix between two different transient processes, as shown with a green dashed line. This separatrix detaches sub- and superthreshold zones in the phase plane. The smaller ellipse for $\varepsilon = 0.01$ totally belongs to the subthreshold zone. This arrangement predicts that random trajectories are localized near the equilibrium M_1. Under increasing noise, the confidence ellipse enlarges. The larger ellipse for $\varepsilon = 0.05$ partially occupies the superthreshold zone. Such arrangement predicts that random trajectories can fall into the superthreshold zone and exhibit large-amplitude loops. Abilities of such a geometrical analysis by confidence ellipses are demonstrated in Fig. 9(b) for $p = 0.5$.

Comparing Figs. 9(a) and 9(b) with Figs. 4(b) and 4(c), we see a good agreement of our analytical prognosis and results of direct numerical simulation.

B. Stochastic excitement in the parameter zone $p > p_6$

Consider now the parameter zone $p > p_6$ where the deterministic system has the only equilibrium M_3 that is stable. Here, in contrast to the previous case $p < p_2$, the arrangement of sub- and superthreshold zones in the phase plane is defined by another separatrix in the form of the transient semiattractor [see discussion of Fig. 3(d)].

The noise-induced transformation of small-amplitude fluctuations around M_3 into the regime of large-amplitude oscillations is shown in Fig. 10 for $p = 1.12$ and $p = 1.5$. Comparing with Fig. 4, one can conclude that random disturbances result not only in the sharp growth of the calcium concentration c but also decrease it.

The results of the analysis of statistics of interspike intervals are presented in Fig. 11. In Fig. 11(a), it is clearly seen how the threshold noise intensity corresponding to the onset of spiking oscillations depends on the parameter p. As for the phenomenon of coherence resonance, in this p-parameter zone it is not accented [see Fig. 11(b)].

Consider now how the confidence domains method works in this case to predict noise-induced excitement. The

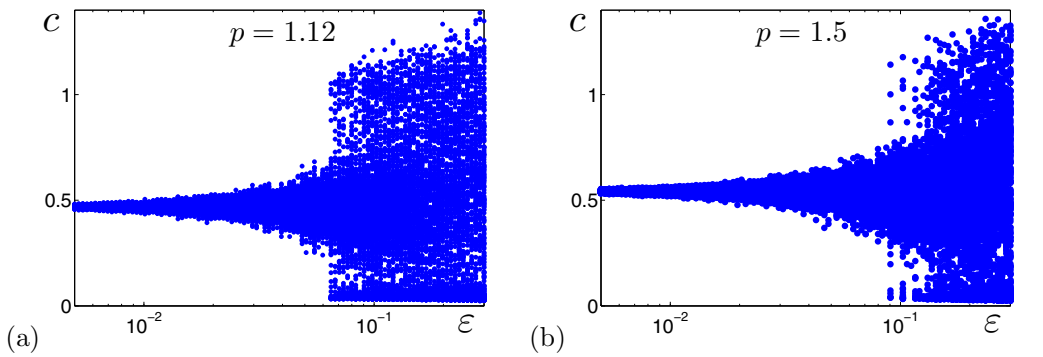

FIG. 10. Random states of the system (2) solutions starting from the equilibrium M_3.

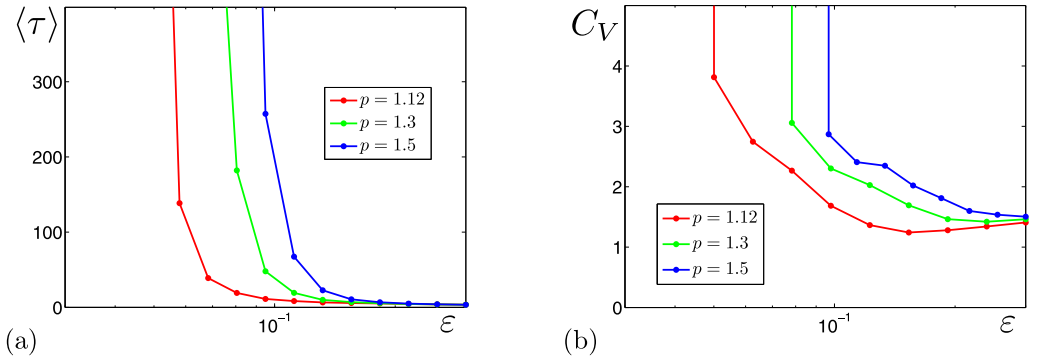

FIG. 11. Mean values $\langle\tau\rangle$ and coefficient of variation C_V of interspike intervals τ versus noise intensity ε in the parameter zone $p > p_6$.

results of direct numerical simulation of random solutions of the system (2) with $p = 1.12$ for $\varepsilon = 0.02$ (red) and $\varepsilon = 0.08$ (green) are presented in Figs. 12(a) and 12(b). As can be seen, at low noise with $\varepsilon = 0.02$, random solutions are localized near the equilibrium M_3. For $\varepsilon = 0.08$, trajectories leave this equilibrium and show large-amplitude stochastic loops near the deterministic semiattractor. The time series [see Fig. 12(b)] show spike-type temporal excitement.

The confidence domains method for $p = 1.12$ is illustrated in Fig. 12(c). Here, we show the phase trajectory of the deterministic system by blue solid lines, and confidence ellipses by dashed lines. The intersection of the confidence ellipse for $\varepsilon = 0.08$ with the transient semiattractor signals about the onset of excitement of spiking calcium oscillations. Comparing Figs. 12(a)–12(c), one can see a good agreement of our analytical prognosis and results of direct numerical simulation.

IV. CONCLUSION

This study is devoted to the problem of identification and analysis of the mechanisms of the genesis of calcium oscillations on the basis of mathematical models. We focus on the question of how the inevitably present random disturbances can generate spike oscillations in parametric zones, where the original deterministic models demonstrate only stable equilibrium regimes. For illustration of the key stochastic phenomena and methods of their analysis, a two-dimensional randomly forced conceptual Li-Rinzel model of calcium dynamics was

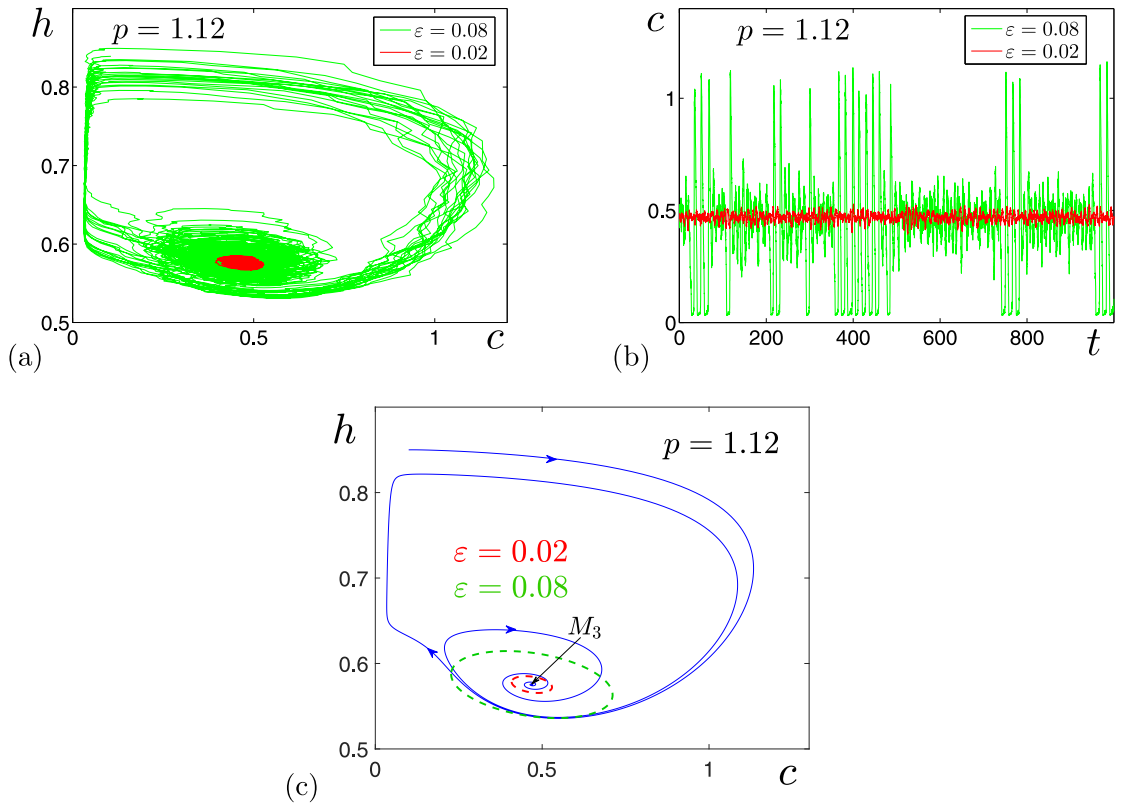

FIG. 12. Random trajectories and time series of the system (2) for $p = 1.12$.

used. When the inositol trisphosphate IP_3 concentration p is varied, the original deterministic model has both self-oscillation zones and adjacent zones of stable equilibria. Using direct numerical simulation, it was shown how in the equilibria p zones, with increasing noise intensity, the system passes from the mode of low-amplitude random fluctuations near equilibria to large-amplitude spike-type oscillations. The statistical analysis of interspike intervals presented here for this stochastic excitability showed a presence of the phenomenon of coherence resonance in one of the two considered p-parametric zones. We discussed how the phenomenon of stochastic excitability is associated with the geometric features of the phase portrait of the original deterministic model, namely, with the presence of sub- and supercritical regions, the transitions between which generate spike transients. Here, the location of the separatrix detaching these regions plays an important role in the parametric analysis of noise-induced excitement of calcium oscillations. In the Li-Rinzel model under consideration, the role of such a separatrix is played by the stable manifold of the nearest saddle equilibrium for one excitability p zone and the transient semiattractor for another one. For the analytical study of the noise-induced transition of the system to the spike excitation mode, it was proposed to use the method of confidence regions. A preliminary estimate of the stochastic sensitivity of equilibria allows one to determine the configuration and size of the confidence ellipses approximating the dispersion of random states. It was shown how the demonstrative geometric analysis of the mutual arrangement of confidence ellipses and separatrices makes it possible to predict the transition of the system from the equilibrium regime to the mode of spike oscillations. The described approach, illustrated in detail by the example of the Li-Rinzel model, can be applied to the analysis of mechanisms of stochastic generation of calcium oscillations in other, more complex models.

ACKNOWLEDGMENT

This work was supported by Russian Science Foundation (Grant No. 21-11-00062).

[1] H. Streb, R. F. Irvine, M. J. Berridge, and I. Schulz, Release of Ca^{2+} from a nonmitochondrial intracellular store in pancreatic acinar cells by inositol-1,4,5-trisphosphate, Nature (London) **306**, 67 (1983).

[2] A. Fabiato, Calcium-induced release of calcium from the cardiac sarcoplasmic reticulum, Am. J. Physiol. **245**, C1 (1983).

[3] M. J. Berridge, Calcium oscillations, J. Biol. Chem. **265**, 9583 (1990).

[4] R. W. Tsien and R. Y. Tsien, Calcium channels, stores, and oscillations, Annu. Rev. Cell. Biol. **6**, 715 (1990).

[5] M. J. Berridge, M. D. Bootman, and H. L. Roderick, Calcium signalling: Dynamics, homeostasis and remodelling, Nat. Rev. Mol. Cell. Biol. **4**, 517 (2003).

[6] J. W. Putney and G. S. Bird, Cytoplasmic calcium oscillations and store-operated calcium influx, J. Physiol. **586**, 3055 (2008).

[7] G. W. De Young and J. Keizer, A single-pool inositol 1,4,5-trisphosphate-receptor-based model for agonist-stimulated oscillations in Ca^{2+} concentration, Proc. Natl. Acad. Sci. USA **89**, 9895 (1992).

[8] S. Schuster, M. Marhl, and T. Hofer, Modelling of simple and complex calcium oscillations. From single-cell responses to intercellular signalling, Eur. J. Biochem. **269**, 1333 (2002).

[9] K. Tsaneva-Atanasova, *A Mathematical Study of Calcium Oscillations and Waves* (VDM Verlag, Saarbrücken, 2009).

[10] G. Dupont, *Models of Calcium Signalling* (Springer Science, New York, 2016).

[11] Y.-X. Li and J. Rinzel, Equations for $InsP_3$ receptor-mediated $[Ca^{2+}]i$ oscillations derived from a detailed kinetic model: A Hodgkin-Huxley like formalism, J. Theor. Biol. **166**, 461 (1994).

[12] G. Dupont and A. Goldbeter, One-pool model for Ca^{2+} oscillations involving Ca^{2+} and inositol 1,4,5-trisphosphate as co-agonists for Ca^{2+} release, Cell Calcium **14**, 311 (1993).

[13] M. De Pittá, V. Volman, H. Levine, G. Pioggia, D. De Rossi, and E. Ben-Jacob, Coexistence of amplitude and frequency modulations in intracellular calcium dynamics, Phys. Rev. E **77**, 030903(R) (2008).

[14] M. Perc, A. K. Green, C. J. Dixon, and M. Marhl, Establishing the stochastic nature of intracellular calcium oscillations from experimental data, Biophys. Chem. **132**, 33 (2008).

[15] K. Thurley, S. C. Tovey, G. Moenke, V. L. Prince, A. Meena, A. P. Thomas, A. Skupin, C. W. Taylor, and M. Falcke, Reliable encoding of stimulus intensities within random sequences of intracellular Ca^{2+} spikes, Sci. Signal **7**, ra59 (2014).

[16] W. Horsthemke and R. Lefever, *Noise-Induced Transitions* (Springer, Berlin, 1984).

[17] F. Moss and P. V. E. McClintock, *Noise in Nonlinear Dynamical Systems* (Cambridge University Press, Cambridge, UK, 1989).

[18] V. S. Anishchenko, V. V. Astakhov, A. B. Neiman, T. E. Vadivasova, and L. Schimansky-Geier, *Nonlinear Dynamics of Chaotic and Stochastic Systems. Tutorial and Modern Development* (Springer-Verlag, Berlin, Heidelberg, 2007).

[19] M. D. McDonnell, N. G. Stocks, C. E. M. Pearce, and D. Abbott, *Stochastic Resonance: From Suprathreshold Stochastic Resonance to Stochastic Signal Quantization* (Cambridge University Press, Cambridge, UK, 2008).

[20] L. Gammaitoni, P. Hanggi, P. Jung, and F. Marchesoni, Stochastic resonance, Rev. Mod. Phys. **70**, 223 (1998).

[21] J. B. Gao, S. K. Hwang, and J. M. Liu, When Can Noise Induce Chaos?, Phys. Rev. Lett. **82**, 1132 (1999).

[22] F. Gassmann, Noise-induced chaos-order transitions, Phys. Rev. E **55**, 2215 (1997).

[23] B. Lindner, J. Garcia-Ojalvo, A. Neiman, and L. Schimansky-Geier, Effects of noise in excitable systems, Phys. Rep. **392**, 321 (2004).

[24] A. N. Pisarchik and R. Jaimes-Reátegui, Deterministic coherence resonance in coupled chaotic oscillators with frequency mismatch, Phys. Rev. E **92**, 050901(R) (2015).

[25] M. A. García-Vellisca, A. N. Pisarchik, and R. Jaimes-Reátegui, Experimental evidence of deterministic coherence resonance in coupled chaotic systems with frequency mismatch, Phys. Rev. E **94**, 012218 (2016).

[26] S. Boccaletti, A. N. Pisarchik, C. I. del Genio, and A. Amann, *Synchronization: From Coupled Systems to Complex Networks* (Cambridge University Press, Cambridge, UK, 2018).

[27] A. S. Pikovsky and J. Kurths, Coherence Resonance in a Noise-Driven Excitable System, Phys. Rev. Lett. **78**, 775 (1997).

[28] I. Bashkirtseva, A. B. Neiman, and L. Ryashko, Stochastic sensitivity analysis of the noise-induced excitability in a model of a hair bundle, Phys. Rev. E **87**, 052711 (2013).

[29] A. V. Andreev, V. V. Makarov, A. E. Runnova, A. N. Pisarchik, and A. E. Hramov, Coherence resonance in stimulated neuronal network, Chaos, Solitons Fractals **106**, 80 (2018).

[30] A. N. Pisarchik, V. A. Maksimenko, A. V. Andreev, N. S. Frolov, V. V. Makarov, M. O. Zhuravlev, A. E. Runnova, and A. E. Hramov, Coherent resonance in the distributed cortical network during sensory information processing, Sci. Rep. **9**, 18325 (2019).

[31] R. Jaimes-Reátegui, J. H. García-López, A. Gallegos, G. Huerta Cuellar, P. Chholak, and A. N. Pisarchik, Deterministic coherence and anti-coherence resonances in networks of chaotic oscillators with frequency mismatch, Chaos, Solitons Fractals **152**, 111424 (2021).

[32] J. W. Shuai and P. Jung, Optimal Intracellular Calcium Signaling, Phys. Rev. Lett. **88**, 068102 (2002).

[33] J. W. Shuai and P. Jung, Stochastic properties of Ca^{2+} release of inositol 1,4,5-trisphosphate receptor clusters, Biophys. J. **83**, 87 (2002).

[34] M. Falcke, On the role of stochastic channel behavior in intracellular Ca^{2+} dynamics, Biophys. J. **84**, 42 (2003).

[35] G. Moenke, M. Falcke, and K. Thurley, Hierarchic stochastic modelling applied to intracellular Ca^{2+} signals, PLoS ONE **7**, e51178 (2012).

[36] J. Powell, M. Falcke, A. Skupin, T. C. Bellamy, T. Kypraios, and R. Thul, in *Calcium Signaling. Advances in Experimental Medicine and Biology* (Springer, New York, 2020), Vol. 1131, pp. 799–826.

[37] L. Ryashko, I. Bashkirtseva, and O. Solovyova, Stochastic dynamics in the Li-Rinzel calcium oscillation model, *Mathematical Methods in the Applied Sciences* (Wiley Online Library, 2021).

[38] Y. P. Li and Q. S. Li, Internal stochastic resonance under two-parameter modulation in intercellular calcium ion oscillations, J. Chem. Phys. **120**, 8748 (2004).

[39] H. Li, Z. Hou, and H. Xin, Internal noise stochastic resonance for intracellular calcium oscillations in a cell system, Phys. Rev. E **71**, 061916 (2005).

[40] W.-L. Duan, F. Long, and C. Li, Reverse resonance and stochastic resonance in intracellular calcium oscillations, Phys. A (Amsterdam, Neth.) **401**, 52 (2014).

[41] J. Ma and Q. Gao, Two types of coherence resonance in an intracellular calcium oscillation system, Chem. Phys. **495**, 29 (2017).

[42] I. Bashkirtseva and L. Ryashko, Constructive analysis of noise-induced transitions for coexisting periodic attractors of Lorenz model, Phys. Rev. E **79**, 041106 (2009).

[43] I. Bashkirtseva, G. Chen, and L. Ryashko, Analysis of noise-induced transitions from regular to chaotic oscillations in the Chen system, Chaos **22**, 033104 (2012).

[44] I. Bashkirtseva, L. Ryashko, and E. Slepukhina, Noise-induced oscillation bistability and transition to chaos in FitzHugh-Nagumo model, Fluctuation Noise Lett. **13**, 1450004 (2014).

[45] I. Bashkirtseva and L. Ryashko, Generation of mixed-mode stochastic oscillations in a hair bundle model, Phys. Rev. E **98**, 042414 (2018).

[46] G. Benettin and L. Galgani, *Intrinsic Stochasticity in Plasmas* (Ecole Polytechnique, Palaiseau, France, 1979), pp. 93–114.

[47] C. Skokos, The Lyapunov characteristic exponents and their computation, in *Dynamics of Small Solar System Bodies and Exoplanets*, edited by J. J. Souchaym and R. Dvorak, Lecture Notes in Physics (Springer, Berlin, Heidelberg, 2010), Vol. 790, pp. 63–135.